

## USE OF ADIPOSE-DERIVED STEM CELLS TO FABRICATE SCAFFOLDLESS TISSUE-ENGINEERED NEURAL CONDUITS *IN VITRO*

A. M. ADAMS,<sup>a</sup> E. M. ARRUDA<sup>b,c,d</sup> AND L. M. LARKIN<sup>a,c,\*</sup>

<sup>a</sup>Department of Molecular and Integrative Physiology, University of Michigan, Ann Arbor, MI 48109, USA

<sup>b</sup>Department of Mechanical Engineering, University of Michigan, Ann Arbor, MI 48109, USA

<sup>c</sup>Department of Biomedical Engineering and University of Michigan, Ann Arbor, MI 48109, USA

<sup>d</sup>Program in Macromolecular Science and Engineering, University of Michigan, Ann Arbor, MI 48109, USA

**Abstract**—Peripheral nerve injuries resulting from trauma or disease often necessitate surgical intervention. Although the gold standard for such repairs uses nerve autografts, alternatives that do not require invasive harvesting of autologous nerve tissues are currently being designed and evaluated. We previously established the use of scaffoldless engineered neural conduits (ENCs) fabricated from primary cells as one such alternative in sciatic nerve repair in rats [Baltich et al. (2010) *In Vitro Cell Dev Biol Anim* 46(5):438–444]. The present study establishes protocols for fabricating neural conduits from adipose-derived stem cells (ASCs) differentiated to either a fibroblast or neural lineage and co-cultured into a three-dimensional (3-D) scaffoldless tissue-ENC. Addition of ascorbic acid-2-phosphate and fibroblast growth factor (FGF)-2 to the medium induced and differentiated ASCs to a fibroblast lineage in more than 90% of the cell population, as confirmed by collagen I expression. ASC-differentiated fibroblasts formed monolayers, delaminated, and formed 3-D conduits. Neurospheres were formed by culturing ASCs on non-adherent surfaces in serum-free neurobasal medium with the addition of epidermal growth factor (EGF) and FGF-2. The addition of 10 ng EGF and 10 ng FGF-2 produced larger and more numerous neurospheres than treatments of lower EGF and FGF-2 concentrations. Subsequent differentiation to glial-like cells was confirmed by the expression of S100. ASC-derived fibroblast monolayers and neurospheres were co-cultured to fabricate a 3-D scaffoldless tissue-ENC. Their nerve-like structure and incorporation of glial-like cells, which would associate with regenerating axons, may make these novel, stem cell-derived neural conduits an efficacious technology for repairing critical gaps following peripheral

nerve injury. © 2011 IBRO. Published by Elsevier Ltd. All rights reserved.

**Key words:** adipose-derived stem cells (ASC), peripheral nerve repair, nerve conduit, tissue engineering.

Peripheral nerve trauma affects 1 in 1000 people resulting in tissue morbidity and decreased quality of life (Shokouhi et al., 2008). These traumas can lead to gaps of damaged nerve tissue between viable nerve sections, which result in a loss of function. Although less significant injuries can be repaired without surgical intervention, injuries that lead to critical nerve gaps require grafts to direct neural regeneration. Autologous nerve grafts from either hosts (autograft) or non-hosts (allograft) are capable of bridging large nerve gaps (Ray and Mackinnon 2010). Autologous nerve grafts are considered the “gold standard” for repairing transected nerves in the peripheral nervous system (Lundborg, 1988; Meek and Coert, 2007; Schmidt and Leach, 2003). However, autologous nerve grafts possess several limitations. The process of harvesting an autograft involves a separate surgical procedure and can lead to loss of function, donor site neuroma, pain, and scarring (Taras et al., 2005). Additionally, there is a finite amount of nerve tissue available for grafting (Millesi, 1991). In contrast, allografts may lead to complications associated with host rejection (Ray and Mackinnon 2010). Because these limitations, considerable research has been devoted to design alternative technologies to bridge critical nerve gaps. Biological and synthetic conduits have been engineered to possess the attributes of autologous nerve grafts without the limitations of availability, donor site morbidity, and the need for two surgical procedures (Taras et al., 2005).

To overcome the limitations of both grafts and current scaffold-based conduit alternatives, our laboratory has previously fabricated three-dimensional (3-D) scaffoldless engineered neural conduits (ENCs) using primary fibroblasts and embryonic-derived neural cells (Baltich et al., 2010). The ENC is similar in structure to native nerve, consisting of a connective tissue exterior sheath and an inner nerve network. The efficacy of the scaffoldless 3-D ENCs in allowing axonal regeneration across a 10-mm nerve gap in the tibial nerve of adult Fisher F344 rats has been evaluated. Although the ENC allowed for axonal regeneration through the 10-mm nerve gap, it was not as efficacious as an autograft in repairing the injured site but nevertheless succeeded in demonstrating a proof of concept of scaffoldless neural cell approaches to nerve repair. Fetal cells are not a relevant cell source for translating these technologies to the clinic; therefore, our laboratory

\*Correspondence to: L. M. Larkin, Department of Molecular and Integrative Physiology and Biomedical Engineering, University of Michigan, Biomedical Science Research Building (BSRB), 109 Zina Pitcher Place, Room 2025, Ann Arbor, MI 48109–2200. Tel: +1-734-936-8181; fax: +1-734-615-3292.

E-mail address: llarkin@umich.edu (L. M. Larkin).

**Abbreviations:** AA2P, ascorbic acid-2-phosphate; ABAM, antibiotic/antimycotic; aENC, adipose-derived stem cell engineered fibroblast conduit; ASC, adipose-derived stem cells; Col1, collagen 1; CSA, cross-sectional area; DM, differentiation medium; DPBS, Dulbecco's phosphate-buffered saline; EDTA, ethylenediaminetetraacetic acid; EGF, epidermal growth factor; ENC, engineered neural conduits; FBS, fetal bovine serum; FGF, fibroblast growth factor; GM, growth medium; MSC, mesenchymal stem cell; NBM, neural basal medium; PFA, paraformaldehyde; T<sub>d</sub>, doubling time; TGF, transforming growth factor; 3-D, three-dimensional.

shifted focus to the fabrication of ENC's from differentiated adipose-derived stem cells (ASCs). Both embryonic-derived neural cells and ASCs eliminate the need for autograft harvesting. ASCs additionally offer a clinically relevant option.

Mesenchymal stem cells (MSCs) are adult marrow-derived and non-marrow-derived stem cells noted for their capability to differentiate into multiple tissue lineages. Although bone marrow was the original and most common site for isolating MSCs, stem cell investigations have undergone a paradigm shift with current research focusing on the isolation, characterization, and use of ASCs as a cell source for tissue engineering (Mosna et al., 2010; Zhu et al., 2008). Characterization of MSC cell surface markers varies with the tissue harvested (adipose-derived tissue vs. bone marrow-derived tissue), and variability has been shown between research groups (Mosna et al., 2010). However, bone marrow-derived stem cells have typically been consistent in positive expression of CD90, CD105, and CD73. The level of expression of these markers in ASCs has not been consistent or reliable for identification. Recently, it has been suggested that surface marker CD271 (p75NTR) is not only located on both adipose- and bone marrow-derived stem cells but could also be used as a sole identifying marker for these cells from the heterogeneous population of cells isolated from bone marrow or adipose fat pads (Griesche et al., 2010; Flores-Torales et al., 2010).

In both animal and human trials, ASCs have been shown to have promising repair potential. ASCs are currently being investigated in trials involving tissue healing after radiotherapy and treatment of recurrent Crohn's fistulae (Locke et al., 2009). Undifferentiated ASCs have been shown to increase nerve regeneration in conduit-based peripheral nerve repair studies (Santiago et al., 2009). Additionally, differentiated ASCs are being evaluated as fat grafts in reconstruction therapies, as bone grafts in osseous defects, as chondrogenic grafts in joint disease and cartilage regeneration treatments, and as neuronal support in regeneration of axons in the peripheral nervous system resulting from peripheral nerve injuries and deficits in the CNS caused by cerebral ischemia (Locke et al., in press). In some cases, the incorporation of ASC-derived neural cells into conduits restored nerve function better than conduits incorporated with Schwann cells (di Summa et al., 2011).

The purpose of this study was to permanently induce ASCs to fibroblast and neural lineages and to co-culture these cells to fabricate and characterize an ENC derived solely from ASCs. This study combines the approach of using stem cells in nerve repair technologies with a recently developed technique from our laboratory for fabricating scaffoldless neural conduits (Radtke et al., 2009; Baltich et al., 2010). In this study, we demonstrate the differentiation of ASCs to fibroblastic and neural lineages, establishment of a co-culture of both cell types, and co-culture fabrication into a 3-D scaffoldless ENC.

## EXPERIMENTAL PROCEDURES

### Animals and animal care

Female Fischer 344 retired breeder rats (Charles River Laboratories, Wilmington, MA, USA) were used to obtain subcutaneous inguinal adipose fat deposits. All rats were acclimated to the established light cycle, temperature, and feeding schedules of our animal colony for 1 week before tissue dissection. All animal care and animal dissections were in accordance with the Guide for Care and Use of Laboratory Animals, limiting the number of animals used as well as any associated pain (Public Health Service, 19965, NIH Publication No. 85-23).

### Isolation of ASCs

The ASC isolation protocol is derived from the isolation techniques described in Yamamoto et al. (2007) and Gronthos et al. (2001). Briefly, excised adipose tissue was stored in a transfer medium (TM) [Dulbecco's phosphate-buffered saline (DPBS, Invitrogen), 2% antibiotic/antimycotic (ABAM, Invitrogen)] and placed in an ice bath until processed. The adipose tissue was removed from the TM and rinsed in 70% EtOH and DPBS. After rinsing, the adipose tissue was finely minced using forceps and a razor blade. The minced tissue was then placed in dissociation medium (DM) [DPBS, 1% trypsin (0.25%)/EDTA (Invitrogen) and 0.1% collagenase I (Invitrogen) filtered through a 0.22  $\mu\text{m}$  Steriflip (Millipore)] and set in a 37° shaking water bath for 20 min. Once dissociation was complete, the buoyant top layer, containing undissociated adipose tissue, was removed and the remnant was filtered through a 70- $\mu\text{m}$  mesh filter. The sample was then centrifuged at 500 $\times g$  for 10 min, the supernatant was aspirated, and the pellet was resuspended in growth medium (GM) [Dulbecco's modified eagle medium (DMEM, Invitrogen), 20% fetal bovine serum (FBS, Invitrogen); 1% ABAM] supplemented with 6 ng/ml fibroblast growth factor (FGF)-2 (PeproTech). The cell suspension was preplated for 4 h at which point the medium was changed, removing and discarding non-adherent cells. This ASC passage 0 culture was refed 4 days later with FGF-2-supplemented GM. The ASC culture was then fed FGF-2-supplemented GM every other day until the monolayer became >90% confluent at which point the cells were passaged. The purity of the cell population was promoted by repeated passaging and by forcefully rinsing the newly seeded ASCs within the first few hours after passaging to allow for the more adherent cells to attach as recommended (Locke et al., in press). ASCs were passaged three times before being used in any differentiation protocol. Undifferentiated ASCs at passage 3 were fixed and assessed for the expression of cell surface markers CD90 and CD271.

Undifferentiated ASCs were continually passaged in GM supplemented with 6 ng/ml FGF-2 until they were induced into a fibroblast or nerve lineage as described later. To test the rate of proliferation when FGF-2 was supplemented in the GM, 50,000 undifferentiated ASCs were seeded in a 48-well plate and given GM with and without FGF-2. To allow the ASCs to reach their first logarithmic growth phase, ASCs were fed for 4 days before being counted (Zhu et al., 2008). The doubling time ( $T_d$ ) was assessed to determine the rate of proliferation.  $T_d$  was calculated using time of seeding ( $t_1$ ), time of assessment ( $t_2$ ), seeding cell density ( $q_1$ ), and living cells at  $t_2$  ( $q_2$ ) in the following equation.

$$T_d = (t_2 - t_1) \bullet \frac{\log 2}{\log(q_2/q_1)}$$

Cell viability was confirmed using Trypan Blue stain (Gibco) during cell counting.

## Fibroblast differentiation

The cell source for fibroblast differentiation was a portion of undifferentiated ASC plates once they had been passaged three times. The ASCs were seeded in 60-mm tissue culture-treated plates at approximately 400,000 cells. ASCs were seeded in GM supplemented with 6 ng/ml FGF-2 and 130  $\mu$ g/ml ascorbic acid-2-phosphate (AA2P) with 50  $\mu$ g/ml proline (Sigma Aldrich). Plates were fed supplemented GM every other day for at least 5 days until the monolayer reached >90% confluence. At this confluence level, several plates of cells were fixed in 4% paraformaldehyde (PFA) and stained for collagen 1 to validate the induction and differentiation into the fibroblast lineage. The remaining plates were used to fabricate conduits.

The optimal concentration of FGF-2 and AA2P to induce ASCs to fibroblasts was evaluated by growing ASCs in GM with different concentrations of both growth factors. The initial concentrations of 6 ng/ml FGF-2 and 130  $\mu$ g/ml AA2P were established previously (Ma et al., 2009). Concentrations of 6, 3, and 0 ng/ml FGF-2 were tested in combination with 130, 65, and 0  $\mu$ g/ml AA2P. Fifty thousand undifferentiated ASCs were seeded in a 48-well plate and fed GM with FGF-2 and AA2P for 3 days at which time plates were fixed with 4% PFA and stained for collagen 1 (Col1). Optimal concentrations of FGF-2 and AA2P were determined by measuring the percent of Col1-positive cells produced.

## Adipose-derived stem cell engineered fibroblast conduit (aEFC) fabrication

Following 5–7 days on GM, the fibroblasts became confluent monolayers of cells. Once the ASCs were induced to a fibroblast lineage and reached >90% confluence, the medium was switched to differentiation medium (DM) [DMEM, 7% horse serum (Invitrogen), 1% ABAM] supplemented with 6 ng/ml FGF-2, 130  $\mu$ g/ml AA2P with 50  $\mu$ g/ml proline, and 12 ng/ml transforming growth factor (TGF)- $\beta$ 1 (PeproTech). The supplemented DM was changed every other day for 7–10 days until the edges of the monolayer were observed to start to delaminate as a result of the passive tension of the fibroblasts. If unconstrained, the passive tension in the monolayer would eventually result in full delamination from the plate and contraction into a spherical mass of tissue. However at the onset of delamination, the fibroblast monolayer was transferred to a sylgard-coated dish (WPI), and constraint pins were placed in the dish such that the monolayer rolled into a cylindrical form, which could then be used as a conduit. The monolayer was then held 16–24 mm apart in the dish using minuten constraint pins. The forming aEFCs' were fed GM every other day until the conduits were observed to become taut at which point they were frozen in Tissue Tek (Fisher) and preserved for histology.

## Neurosphere induction

The neurosphere induction protocol was derived from methods used by Radtke et al. (2009) and Bunnell et al. (2008). ASCs were obtained from primary ASC culture at passage 3 or later. ASCs were seeded on Pyrex plates (Falcon) at 1000 cells/ml of neural basal medium (NBM) supplemented with 1% N2 (Invitrogen), 1% ABAM, 1% B27 (Invitrogen), 10 ng/ml epidermal growth factor [EGF (Invitrogen)], and 10 ng/ml FGF-2. N2 and B27 are commonly used, serum-free, growth factor cocktails, which are used to promote and sustain neural growth. Neurosphere cultures were observed for 3 days, replenishing EGF and FGF-2 each day. The concentrations of EGF and FGF-2 needed to induce ASCs to neurospheres were evaluated by observing the amount and size of the neurospheres produced when varying concentrations were added to the induction medium. Fifty thousand undifferentiated ASCs were seeded on sylgard-coated 12-well plates in NBM supplemented with N2, ABAM, B27, and various concentrations of

EGF and FGF-2. On day 3, phase contrast images were taken to assess the count and size of neurospheres. These neurospheres were then transferred to adherent tissue culture-treated dishes to induce glial-like cell differentiation.

To differentiate neurospheres to glial-like cells, free-floating neurospheres were collected and centrifuged at 800 $\times$ g for 10 min. Pelleted neurospheres were resuspended in NBM supplemented with B27. These cultures were fed B27-supplemented NBM every other day for 7–10 days either on tissue culture-treated dishes (then fixed for histology) or on top of an ASC-induced fibroblast monolayer for aENC formation.

Neurosphere differentiation into glial-like cells was accomplished using differentiation medium [(DM), NBM supplemented with 1% B27, 1% ABAM, and 1% N2]. To test the effects of serum and growth factors on neurospheres, experimental treatments were fed DM with 10% FBS, DM with 10 ng/ml EGF and 10 ng/ml FGF-2, or serum-based GM. The neurospheres were fed DM for 3 days at which point the neurospheres were assessed for ability to attach and extend neural processes. Successful differentiation was determined by the size and number of neurospheres produced as well as the presence of neural processes and neural marker S100.

## aENC fabrication

After ASC-induced fibroblast monolayers reached >80% confluence on GM, neurospheres were seeded on top of them. The co-culture was fed NBM supplemented with B27, so as to allow for expansion of the neural cells while simultaneously arresting the growth of the fibroblasts. After 7–10 days, a neural network was established and the cells were fed FGF-2-supplemented and AA2P-supplemented GM to recover the fibroblasts. After ~3 days, the medium was switched to TGF- $\beta$ 1-supplemented and AA2P-supplemented DM, as in the case of the aEFCs. The supplemented DM was changed every other day for 7–10 days until the edges of the monolayer were observed to start to delaminate, at which point the monolayer was manually formed into a cylinder, transferred to a sylgard-coated dish, and pinned in place. Once pinned, the aENCs were fed GM until taut, at which point they were frozen in Tissue Tek and preserved for histology.

## Histology

For immunohistochemical analysis, cell populations were rinsed in DPBS (three times for 10 min each) then fixed with 4% PFA for 45 min. Cells were permeabilized with 0.2% Triton X-100 (Sigma) for 10 min, followed by a 30 min blocking step in 5% donkey serum (Sigma). Cells were incubated overnight at 4 °C with primary antibodies [Col1, S100 (Santa Cruz), CD90, or CD271 (Abcam)] at a dilution of 1:100. They were then incubated with AlexaFluor 488- or 555-conjugated secondary antibodies (Abcam) for 1 h at room temperature, followed by incubation with 2% DAPI for 5 minutes. Fluorescent and phase images were acquired using a Leica DMIRB inverted microscope fitted with an Olympus DP30BW high-sensitivity gray-scale CCD camera. Images were captured at 5 $\times$ , 10 $\times$ , or 40 $\times$  objectives.

## Statistics

Statistical comparisons were performed using values of means $\pm$ standard error (SE) to determine statistical significance. When two groups were compared, the student's *T*-test was performed. Comparisons of three groups or more were performed by one-way ANOVA tests. Statistical significance was recognized at *P*<0.05. Differences yielding a *P*<0.001 were also noted in the figures.

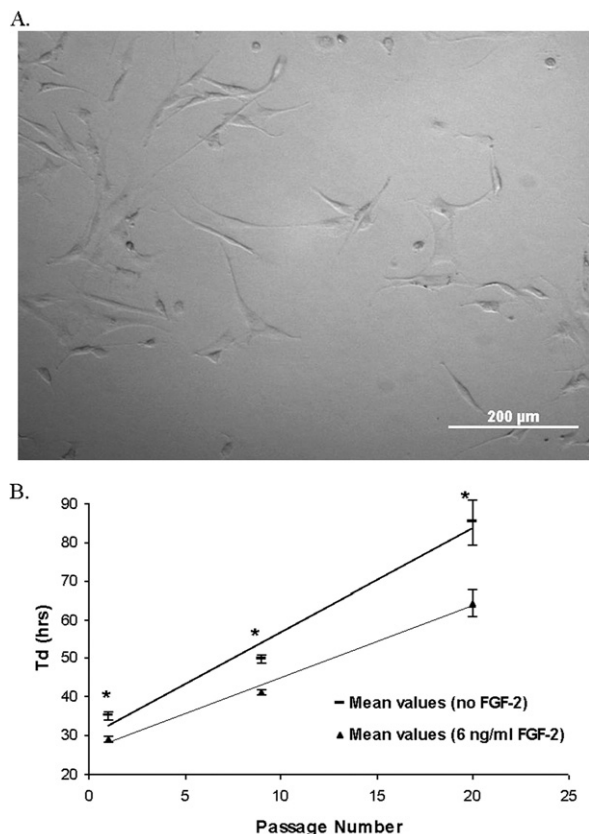


**Fig. 1.** Spindle-shaped morphology of undifferentiated ASCs at passage 3. Phase contrast at 40 $\times$  magnification (A). Doubling time ( $T_d$ ) of ASCs at different passage number and with or without the addition of FGF-2 added to the growth medium (B). The addition of FGF-2 to undifferentiated ASCs significantly decreased their  $T_d$ . The statistical significance of the addition of FGF-2 to undifferentiated ASCs increased in later passages as compared with earlier passages. \*  $P < 0.05$ , compared with treatments with 6 ng/ml FGF-2.

## RESULTS

### Isolation of ASCs

The ASCs were observed to have spindle-shaped morphology, beginning at passage 0 and through passage 12 (Fig. 1). Undifferentiated ASC populations from passage 0 exhibited negative staining for adipocyte dye, Oil Red O (Sigma Aldrich). Immunohistochemical analysis revealed that undifferentiated ASC populations from passage 3 stained positive for surface markers CD90 (98%) and CD271 (96%).

### Optimizing proliferation with FGF-2

Our current protocol uses GM supplemented with FGF-2 to increase the rate of proliferation of the undifferentiated ASCs. Rate of proliferation or  $T_d$  was calculated for proliferation experiments in GM with and without FGF-2. The total cell count after 3 days *in vitro* was taken and compared with the initial seeding density using the  $T_d$  equation (Zhu et al., 2008). The  $T_d$  values were entered on a scatter plot to assess the changes in proliferation rates of ASC populations at passages 1, 9, and 20, both with and with-

out the addition of 6 ng/ml FGF-2 (Fig. 1B). Proliferation was slower for cells at later passages. ASCs, which were given FGF-2, decreased  $T_d$  by 20% in passage 1 and 9, and by 25% in passage 20.

### Fibroblast differentiation

During the induction phase of fibroblast differentiation (between 5 and 7 days) and before reaching confluence, over 90% of the differentiated ASCs expressed the fibroblast marker Col1 (Fig. 2A). The effects of varying concentrations of FGF-2 and AA2P with proline on fibroblast induction and differentiation were quantified by calculating the percentage of cells staining positively for Col1 (Fig. 2C). Treatments with no growth factors or only FGF-2 (6 ng) resulted in a minimal percentage of Col1-positive cells [5–10% (Fig. 2B)]. The addition of 6 ng of FGF-2 increased the Col1-positive cell population to 73%. The treatment using only AA2P (130  $\mu$ g) with proline (50  $\mu$ g) and no FGF-2 increased fibroblast differentiation to 50% Col1-positive cells. Thus, the optimal concentrations of growth factors for differentiation were 130  $\mu$ g of AA2P with 50  $\mu$ g proline and 6 ng FGF-2,

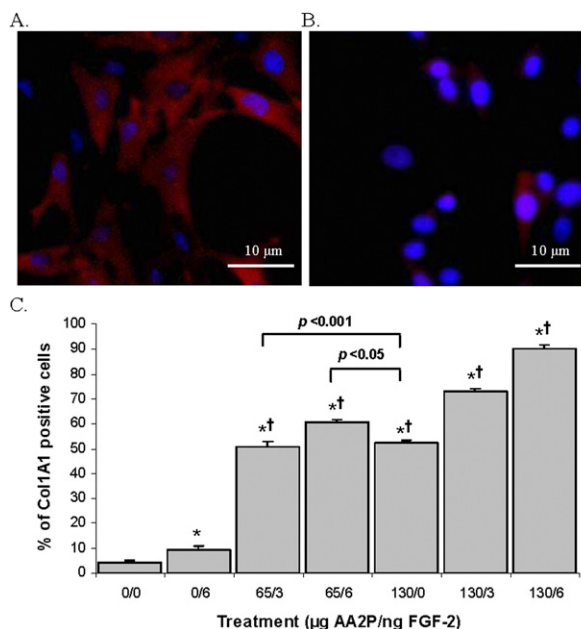


**Fig. 2.** Percentage of ASCs differentiated to fibroblasts. Differentiation of ASCs to fibroblasts was observed by the presence of collagen-1. Col1 (red) and DAPI (blue) at 40 $\times$  magnification in control treatments, given no FGF-2 or ascorbic acid 2-phosphate (A) and in the optimal treatment, given 130  $\mu$ g AA2P and 6 ng FGF-2 (B). Col1-positive cells were counted and compared with the total number of cells using DAPI to determine the percent differentiated (C). Differentiation medium with no FGF-2 and AA2P was used as a negative control, 4%. The addition of just FGF-2 increased the fibroblast differentiation of ASCs to 9%. The addition of any amount of AA2P with or without FGF-2 resulted in 50–60% Col1-positive ASC-induced fibroblasts. Differentiation medium, which included both FGF-2 and AA2P (51–90%), gave rise to significantly more fibroblasts than media with only FGF-2 (9%). \*  $P < 0.05$ , compared with negative control; †  $P < 0.05$ , compared with treatment with no AA2P and 6 ng/ml FGF-2. For interpretation of the references to color in this figure legend, the reader is referred to the Web version of this article.

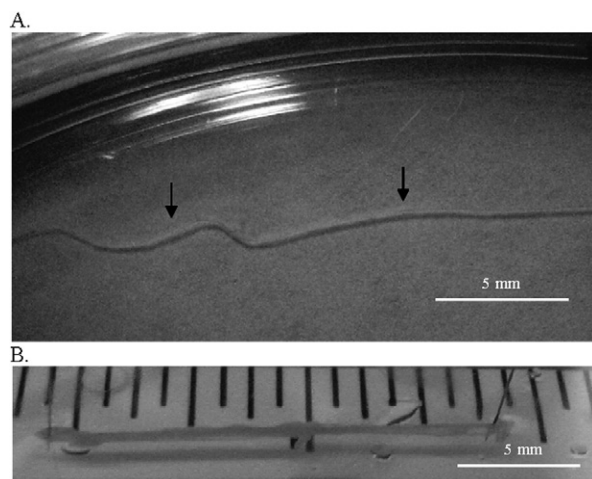


**Fig. 3.** Delamination (marked by arrows) of the ASC-derived fibroblast monolayer from the edges of the tissue culture plate (A). Three-dimensional formation of aEFC (engineered fibroblast conduit fabricated only from ASC-derived fibroblasts) at 16 mm length *in vitro* held in place by constraint pins (B).

which resulted in 90% Col1-positive cells. Once confluent and fed DM, the fibroblast monolayer was observed undergoing delamination due to the switch to low serum media (Fig. 3A). The monolayer was manually formed into a cylinder and held in place by constraint pins. The conduit remodeled into a 16–24-mm long fibroblast conduit, referred to as an aEFC (Fig. 3B).

### Neurogenesis

Neurosphere aggregates were observed to form on -adherent Pyrex® plates in EGF- and FGF-2-supplemented

serum-free NBM (Fig. 4A). When transplanted to an adherent surface and fed NBM without supplemented growth factors, the neurospheres attached and formed neural processes (Fig. 4B–D). These glial-like cells were shown to be distinct from the ASC-derived fibroblasts in co-culture, staining negative for Col1 and positive for S100 (Fig. 5B).

Neurosphere induction was tested using nine combinations of 0, 5, and 10 ng/ml of both EGF and FGF-2. The number and cross-sectional area of neurospheres per well were calculated (Fig. 6). When both EGF and FGF-2 were absent from the induction medium, no neurospheres were observed. It was observed that the concentration of 10 ng/ml EGF in combination with 10 ng/ml FGF-2 was optimal for neurosphere induction (Fig. 6). With treatments using less than 10 ng/ml EGF and 10 ng/ml of FGF-2, fewer and smaller neurospheres were observed. Treatments with only EGF supplementation gave rise to larger neurospheres ( $432 \mu\text{m}^2$ ) than treatments with only FGF-2 ( $158 \mu\text{m}^2$ ). The treatments with 10 ng/ml of EGF in combination with either 10 ng/ml or 5 ng/ml of FGF-2 gave rise to the largest neurospheres ( $675\text{--}750 \mu\text{m}^2$ ). However, the treatment with 10 ng/ml of EGF and 10 ng/ml of FGF-2 produced significantly more neurospheres ( $1.06 \times 10^5$ ) than treatments of 10 ng/ml of EGF with only 5 ng/ml of FGF-2 ( $3.75 \times 10^4$ ).

The glial-like cell differentiation of neurospheres was confirmed by the presence of S100-positive cells (Fig. 5B). When neurospheres were seeded in serum-based medium (GM or NBM with 20% FBS), one of two observations was made. Either the cells did not attach to the dish or the resulting cells returned to a spindle-shaped undifferentiated morphology with no processes. Neurospheres

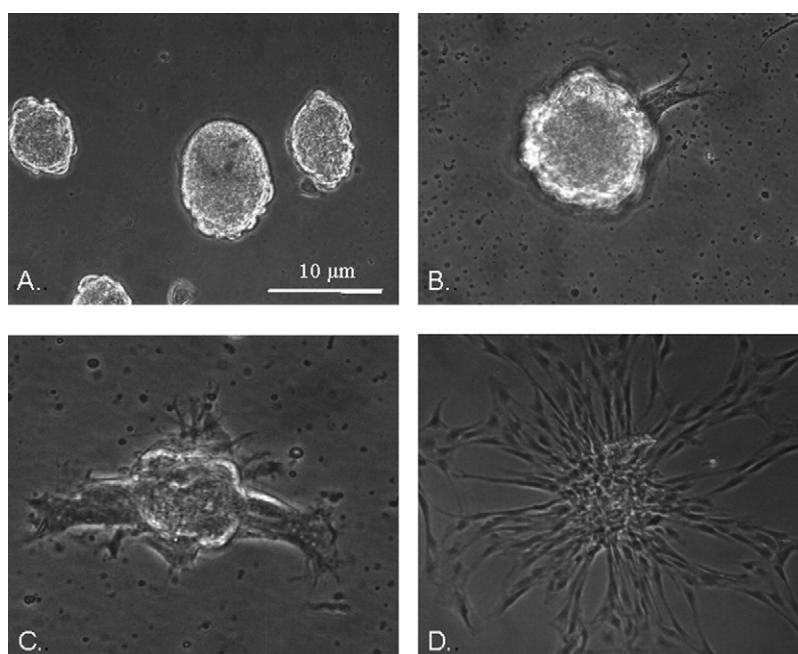


**Fig. 4.** Neurospheres were observed as free-floating aggregates of cells (A), which began to attach 1 d after being transferred to an adherent surface (B). On day 3, more cells were observed attaching to the plate (C). By day 7, nearly all cells from the neurosphere attached to the plate and extended neural processes (D). Phase contrast at 40× magnification.

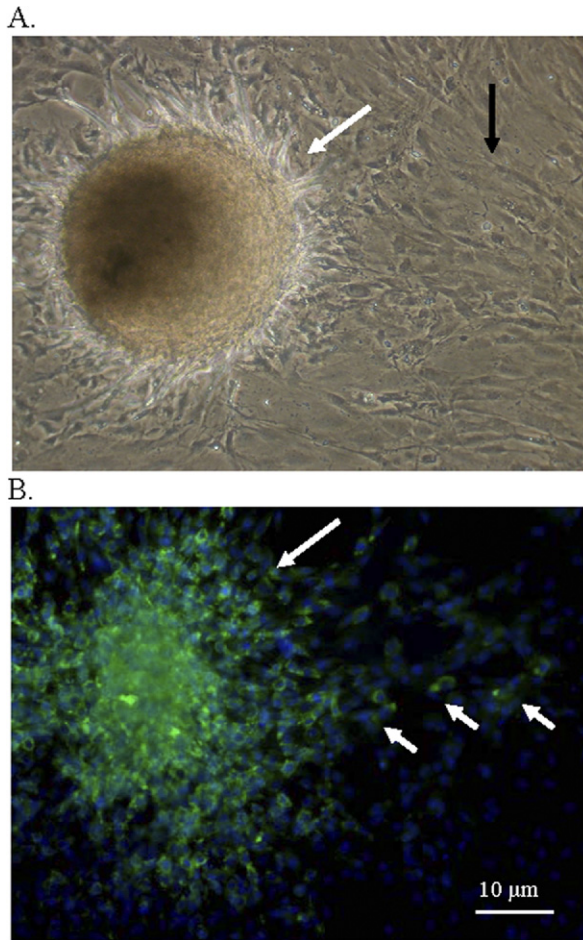


**Fig. 5.** In co-culture with ASC-derived fibroblasts monolayer (black arrow), neurospheres (white arrow) were observed attaching and expanding on the fibroblast monolayer (A). Phase contrast at 40 $\times$  magnification. The glial-like cells (small arrows) coming from the neurosphere (large arrow) migrated onto the fibroblast monolayer as indicated by positive staining for Schwann cell marker S100 (B). S100 (green) and DAPI (blue) at 40 $\times$  magnification. For interpretation of the references to color in this figure legend, the reader is referred to the Web version of this article.

seeded in NBM with EGF and FGF-2 resulted in similar glial-like cells as compared with the neurospheres seeded in only NBM (Fig. 5).

### Conduit formation

Like the aEFC previously described, the co-culture of glial-like cells and ASC-derived fibroblasts delaminated and formed a 3-D ENC, aENC, (Fig. 7A). The length of the aENCs was pre-customized between 20 and 45 mm depending on the size of the dish in which the monolayer was made (Fig. 7A). The thickness of the aENCs was measured at a range of 0.3–1.0 mm. Histology of the aENC was performed 7 days after formation and revealed fibroblasts forming an epineurial-like sheath surrounding an inner neural network (Fig. 7B). The fibroblasts of the aENC stained positive for Col1 and were

observed encasing the conduit as well as throughout the centre. The S100-positive glial-like cells were observed within the conduit.

## DISCUSSION

The purpose of this study was to fabricate and characterize a novel scaffoldless 3-D tissue-ENC composed of ASC. This aENC consisted of an outer sheath of fibroblast cells and an inner network of glial-like neural cells. The use of ASC addresses and eliminates the most limiting factor in successful repair of peripheral nerve injuries, availability of autologous nerve tissue. The ASCs used in the fabrication of the aENC are abundant and biocompatible and thus eliminate the concerns of availability and immune rejection, which are observed with most engineered conduits. Immunohistochemical analysis of the ASC-derived aENC indicates that a 3-D nerve conduit with a fibroblast exterior and interior neural network was successfully engineered. Thus, this scaffoldless 3-D ASC-derived nerve-fibroblast conduit may show potential for replacement of damaged nerve tissue.

Although its adhesive properties facilitated the isolation of ASCs, we confirmed the expression of cell

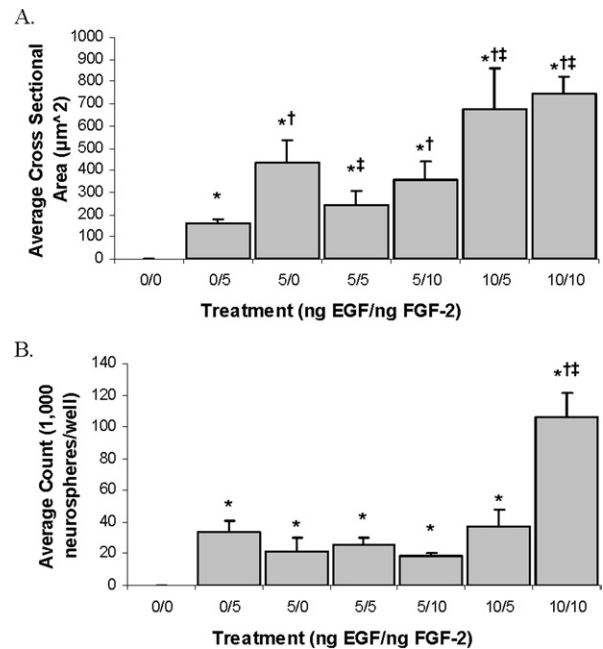


**Fig. 6.** Neurosphere induction at different concentrations of EGF and FGF-2. Between 30 and 80, neurospheres were measured from each treatment to find the average cross-sectional area, CSA (A). Without EGF or FGF-2, no neurospheres accumulated. Treatments with 5 ng of EGF produced neurospheres of a statistically similar CSA with or without the addition of FGF-2. Additionally neurospheres from treatments with 10 ng of EGF had similar CSA whether or not FGF-2 was added. The total number of neurospheres in each well for each treatment was also counted (B). The treatment with 10 ng of both EGF and FGF-2 resulted in significantly more neurospheres per well than any other treatment. All other treatments yielded no significant difference from each other. \*  $P < 0.05$ , compared with negative control; †  $P < 0.05$ , compared with treatment with 0 ng/ml EGF and 5 ng/ml FGF-2; ‡  $P < 0.05$ , compared with treatment with 5 ng/ml EGF and 0 ng/ml FGF-2.

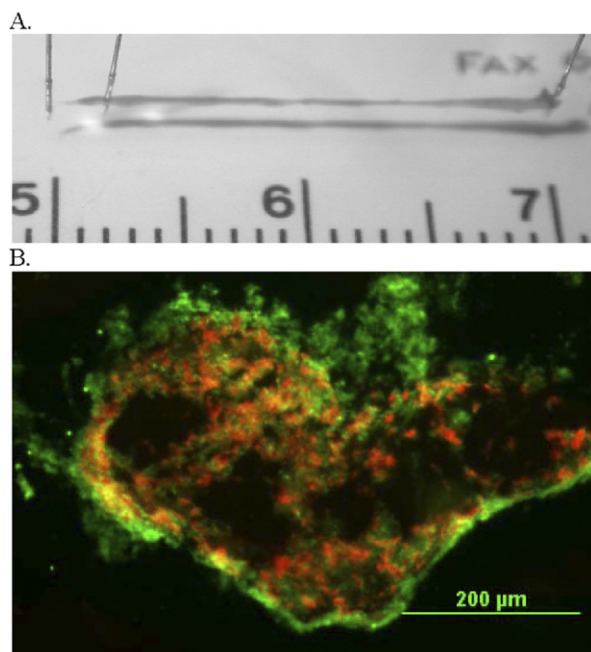


**Fig. 7.** The three-dimensional formation of engineered neural conduit fabricated from ASC-induced fibroblasts and ASC-induced glial-like cells (aENC) at 20 mm length *in vitro* (A). Ruler is in mm. The presence of both fibroblast and glial-like cell types in the aENC cross section were confirmed using collagen marker Col1 (green) and S100 (red) (B). Fibroblasts were observed surrounding an inner neural network. For interpretation of the references to color in this figure legend, the reader is referred to the Web version of this article.

surface markers CD90 and CD271 at passage 3. We decided to use marker CD271, also known as p75NTR, to identify our ASC population because of its supposed potential to be a solely distinguishing marker for ASCs. The presence of the CD90 marker was used to further confirm ASC identification.

Current technologies related to neural tissue engineering focus on using nerve guidance channels for the repair of peripheral nerve injury (Ray and Mackinnon 2010; Deumens et al., 2010). These scaffolded guidance channels are often incorporated with combinations of Schwann cells, stem cells, and neurotrophic factors, which direct and enhance growth of regenerating nerve (Hudson et al., 2000). Although these engineered conduits have found success with small peripheral nerve defects, they are still faced with several drawbacks associated with the use of scaffolds, including biocompatibility, immune rejection, poor cell adhesion, and mediocre tissue repair. The need for a more biocompatible, readily available engineered conduit for repair of larger defects persists. The experiments conducted here present the technology for the development of a scaffoldless 3-D ENC from a readily available, biocompatible source of cells, ASCs, which overcomes the drawbacks associated with current autograft and scaffold-based technologies.

Recent studies have investigated the use of ASCs as a source of support cells incorporated into nerve conduits (Locke et al., in press). The use of these support cells has shown promising yet limited success in enhancing nerve regeneration during peripheral nerve recovery. Use of undif-

ferentiated ASCs in tissue regeneration is difficult to assess because of technical issues leading to permanently inducing ASCs to the appropriate lineage *in vivo*, or apoptosis of ASCs during recovery. Santiago et al. (2009) seeded undifferentiated ASCs in polycaprolactone synthetic conduits and used these conduits to repair small gaps in the sciatic nerve of adult rats. The use of the ASC-incorporated conduit in this repair model showed efficacy in regaining innervation to and preventing atrophy of the target muscle. However, these ASCs were incapable of differentiating solely to a neural lineage. Although few of the ASCs were positive for Schwann cell markers, some cells differentiated to unwanted adipocytes, and many of them remained undifferentiated. The random fates of these ASCs *in vivo* may lead to varied results in terms of nerve recovery.

The use of ASC-induced neural cells in tissue regeneration is difficult because of issues leading to permanently inducing ASCs to the appropriate lineage *in vitro*, prevention of revision of the induced ASCs back to a mesenchymal state *in vivo*, or apoptosis of ASCs either *in vivo* or *in vitro*. In a separate study, di Summa et al. incorporated ASC-included neural cells in a scaffold-based system and implanted them into a peripheral nerve repair (di Summa et al., 2011). These conduits incorporated with ASC-induced neural cells resulted in more robust nerve regeneration and muscle recovery than conduit incorporated with either bone-marrow derived MSCs induced to neural cells or conduits incorporated with primary Schwann cells (di Summa et al., 2011). However,  $\beta$ -mercaptoethanol and forskolin were used to terminally differentiate ASC to a neural lineage. The use of such cytotoxic compounds may not be translationally relevant. In contrast, our scaffoldless technology overcomes these limitations by permanently inducing ASCs to fibroblasts and glial-like cells by using growth factors found naturally in a regenerating tissue such as FGF-2, ascorbic acid, EGF, and TGF- $\beta$ 1. Our methodology presents a more clinically relevant model for conduit technologies used in peripheral nerve repair.

In addition to the potential concerns with terminal differentiation of our ASC cell population, there are issues with the morphology of terminally induced neuronal cells for use in tissue engineering. This concern arises because of the fact that mesenchymal cells induced to a neural lineage very quickly take on a more phenotypically developed morphology, extend neural processes radially from the cell, and attach to the substrate on which the cell is growing. Releasing these neural-induced cells and their neuronal processes to incorporate them into a conduit may damage the processes, lose the integrity of the cell, and lead to apoptosis. Thus, incorporation of neural-induced ASCs before the formation of neuronal processes and attachments was novel and essential for use as a cell source in our conduit approach.

Several laboratories have developed methodologies to induce MSCs to a neural lineage in glass cell culture dishes where the cells remain in suspension and aggregate into free-floating neurospheres (Radtke et al., 2009; Bunnell et al., 2008). When these neurospheres are transferred onto an adherent surface in serum-free medium,

they attach and extend neural processes. To date these neurospheres have only been used *in vitro* to study the proliferation of neural cells from explanted dorsal root ganglia (Radtke et al., 2009). We hypothesized that this neurosphere technology could be applied to our scaffoldless engineered conduit technology such that the co-culture of a fibroblast monolayer seeded with ASC-induced neurospheres would result in the successful fabrication of a functional neural conduit. In our laboratory, we successfully induced ASC to neurospheres. When these neurospheres were co-cultured with a confluent monolayer of fibroblasts, we successfully fabricated a 3-D construct, resulting in the formation of an adipose–cell-derived scaffoldless ENC, or aENC.

## CONCLUSION

We successfully differentiated ASC to fibroblasts and glial-like cells. We were able to co-culture both of these cell types and maintain their distinct cell lineages. Finally, we fabricated scaffoldless 3-D tissue-ENCs from these co-cultures. These conduits have the potential to repair peripheral nerve traumas and represent a novel scaffoldless tissue-engineering technology.

*Acknowledgments*—This research was supported by a NIH, NIAMS, NIBIB funded grant R01 AR054778-02 and from the Barbara and Richard Raynor Medical Foundation Award. We acknowledge Rose Lee and Mike Williams for technical assistance.

## REFERENCES

- Baltich J, Hatch-Vallier L, Adams AM, Arruda EM, Larkin LM (2010) Development of a scaffoldless three-dimensional engineered nerve using a nerve-fibroblast co-culture. *In Vitro Cell Dev Biol Anim* 46(5):438–444.
- Bunnell BA, Estes BT, Guilak F, Gimple JM (2008) Differentiation of adipose stem cells. *Methods Mol Biol* 456:155–171.
- Deumens R, Bozkurt A, Meek MF, Marcus MA, Joosten EA, Weis J, et al. (2010) Repairing injured peripheral nerves: bridging the gap. *Prog Neurobiol* 92(3):245–276.
- di Summa PG, et al. (2011) Long-term *in vivo* regeneration of peripheral nerves through bioengineered nerve grafts. *Neuroscience* 181(5):278–291.
- Flores-Torales E, Orozco-Barocio A, Gonzalez-Ramella OR, Carrasco-Yalan A, Gazarian K, Cuneo-Pareto S (2010) The CD271 expression could be alone for establisher phenotypic marker in Bone marrow derived mesenchymal stem cells. *Folia Histochem Cytobiol* 48(4):682–686.
- Griesche N, Luttmann W, Luttmann A, Stammermann T, Geiger H, Baer PC (2010) A simple modification of the separation method reduces heterogeneity of adipose-derived stem cells. *Cells Tissues Organs* 192(2):106–115.
- Gronthos S, Franklin DM, Leddy HA, Robey PG, Storms RW, Gimple JM (2001) Surface protein characterization of human adipose tissue-derived stromal cells. *J Cell Physiol* 189(1):54–63.
- Hudson TW, Evans GR, Schmidt CE (2000) Engineering strategies for peripheral nerve repair. *Orthop Clin North Am* 31(3):485–498.
- Locke M, Feisst V, Dunbar PR (in press) Concise review: human adipose-derived stem cells (ASC): separating promise from clinical need. *Stem Cells*, in press.
- Locke M, Windsor J, Dunbar PR (2009) Human adipose-derived stem cells: isolation, characterization and applications in surgery. *ANZ J Surg* 79(4):235–244.
- Lundborg G (1988) Nerve injury and repair. New York: Longman.
- Ma J, Goble K, Smietana M, Kostrominova T, Larkin L, Arruda EM (2009) Morphological and functional characteristics of three-dimensional engineered bone-ligament-bone constructs following implantation. *J Biomech Eng* 131(10):101017.
- Meek MF, Coert JH (2007) Synthetic nerve guide implants in humans: a comprehensive survey. *Neurosurgery* 61(6):E1340.
- Millesi H (1991) Indications and techniques of nerve grafting. In: Operative nerve repair and reconstruction (Gelvertman RH, ed), pp 525–544. Philadelphia: Lippincott JB.
- Mosna F, Sensebé L, Krampera M (2010) Human bone marrow and adipose tissue mesenchymal stem cells: a user's guide. *Stem Cells Dev* 19(10):1449–1470.
- Radtke C, Schmitz B, Spies M, Kocsis JD, Vogt PM (2009) Peripheral glial cell differentiation from neurospheres derived from adipose mesenchymal stem cells. *Int J Dev Neurosci* 27(8):817–823.
- Ray WZ, Mackinnon SE (2010) Management of nerve gaps: autografts, allografts, nerve transfers, and end-to-side neurotaphy. *Exp Neurol* 223(1):77–85.
- Santiago LY, Clavijo-Alvarez J, Brayfield C, Rubin JP, Marra KG (2009) Delivery of adipose-derived precursor cells for peripheral nerve repair. *Cell Transplant* 18(2):145–158.
- Schmidt CE, Leach JB (2003) Neural tissue engineering: strategies for repair and regeneration. *Annu Review Biomed Eng* 5:293–347.
- Shokouhi G, Tubbs RS, Shoja MM, Hadidchi S, Ghorbanihaghjo A, Roshangar L, et al. (2008) Neuroprotective effects of high-dose vs low-dose melatonin after blunt sciatic nerve injury. *Childs Nerv Syst* 24(1):111–117.
- Taras JS, Nanavati V, Steelman P (2005) Nerve conduits. *J Hand Ther* 18(2):191–197.
- Yamamoto N, Akamatsu H, Hasegawa S, Yamada T, Nakata S, Okuma M, et al. (2007) Isolation of multipotent stem cells from mouse adipose tissue. *J Dermatol Sci* 48(1):43–52.
- Zhu Y, Liu T, Song K, Fan X, Ma X, Cui Z (2008) Adipose-derived stem cell: a better stem cell than BMSC. *Cell Biochem Funct* 26(6):664–675.